ELSEVIER

Nuclear Instruments and Methods in Physics Research A 450 (2000) 325–337

NUCLEAR INSTRUMENTS & METHODS IN PHYSICS RESEARCH
Section A

www.elsevier.nl/locate/nima

Three-detector setup for positron-lifetime spectroscopy of solids containing ^{60}Co radionuclide

Jakub Čížek*, František Bečvář, Ivan Procházka

Charles University in Prague, Faculty of Mathematics and Physics, Department of Low-Temperature Physics,
V Holešovičkách 2, CZ-180 00 Prague 8, Czech Republic

Received 13 December 1999; received in revised form 10 January 2000; accepted 7 February 2000

Abstract

A three-detector BaF_2 positron-lifetime spectrometer is described. The spectrometer is suited for investigations of the neutron-irradiated reactor pressure vessel steels with a high content of ^{60}Co. Both timing and energy information about annihilation γ-rays is used for selection of coincidence events. In the triple-coincidence mode, the time resolution of around 220 ps FWHM and the coincidence count rate of 15 s^{-1} for a 4 MBq ^{22}Na positron source are simultaneously achieved. Test measurements performed have shown that in this mode the ^{60}Co prompt-peak contribution in the positron-lifetime spectrum is suppressed to be below 1% when ^{60}Co activity of a pair of specimens studied does not exceed the level of 4 MBq. © 2000 Elsevier Science B.V. All rights reserved.

PACS: 78.70.Bj

Keywords: Positron annihilation; Positron-lifetime spectroscopy; Three-detector setup; Neutron-irradiated RPV steels

1. Introduction

The irradiation-induced changes in the mechanical properties of various technologically important materials are subject to a permanent interest of solid-state science and applied research. A special attention is paid to a problem of embrittlement of reactor pressure vessel (RPV) steels. In this case, following a generally accepted opinion, the underlying cause responsible for embrittlement is formation and further evolution of the irradiation-induced small point defect clusters and solute atom precipitates. Vacancies play an important role in the microstructure evolution. As vacancies and their dynamics can be studied with the aid of Positron-Lifetime (PL) spectroscopy, the application of such technique seems also a promising tool for deeper understanding of the irradiation-induced embrittlement process in these critically important materials.

However, application of the PL spectroscopy to investigation of the neutron-irradiated RPV steels is not straightforward. This is because of a considerable amount of the ^{60}Co activity induced in the material during irradiation. For example, a pair of disc-shaped specimens having size of $50\ mm^2 \times 0.2$ mm, which is a typical minimum size required in applications of the PL spectroscopy to metals, may contain up to about 4 MBq of ^{60}Co accumulated after irradiation to a fluence of

---

* Corresponding author.
E-mail address: jcizek@mbox.troja.mff.cuni.cz (J.Čížek).

PII: S0168-9002(00)00277-1

10^{25} m^{-2}. Such a fluence corresponds to a 10 years operation of a VVER 440 nuclear reactor. The ^{60}Co nuclei emit two successive γ-rays with energies of 1.174 and 1.332 MeV. In a standard two-detector PL spectrometer, these γ-rays can activate the start and stop branches of the electronics system. When the conventional ^{22}Na positron source is used, energy windows are usually adjusted at 1274 and 511 keV to suppress this activation. However, in view of a relatively strong role of the Compton scattering in the γ-detection process, even if these windows are choosen very narrow, they will still not provide efficient enough discrimination of the ^{60}Co γ-rays. As a consequence, measurements with samples of RPV steel yield PL spectra in which a false, often dominating prompt peak may appear.

Several ways to tackle the problem of the ^{60}Co prompt-peak interference with the physical part of the PL spectra have been considered so far. In Ref. [1], it was suggested to perform the two measurements of the PL spectra: a standard one with the positron source sandwiched between a pair of the irradiated steel specimens and another one with the positron source removed. The difference spectrum was then considered as the pure PL spectrum with no ^{60}Co contribution. The drawback of such a procedure consists not only in a reduced statistical accuracy, but mainly in substantially non-equivalent conditions at which the two subtracted spectra are collected. Significant shape distortions can be introduced by such a procedure into the difference spectrum [2]. Exclusion of the prompt-peak region from analysis of the measured PL spectrum, as proposed in Ref. [2], would apparently strongly reduce the amount and reliability of the data yielded by the experiment, especially as far as the short-lived components are concerned. Involving the prompt peak directly in the model fitted to the PL spectrum is not sufficient too much, because the shape of the ^{60}Co prompt peak may turn out to be different from the shape of the time resolution function for ^{22}Na [3]. In such a case, lifetimes and relative intensities of spectral components are expected to be appreciably influenced by the chosen shape of ^{60}Co prompt peak and a need for additional free parameters for description of the ^{60}Co prompt peak may arise.

All the above-listed measures can provide only for a partial suppression of the ^{60}Co prompt peak relatively to the true effect created by ^{22}Na positrons. In many cases of interest, these measures appear to be unsatisfactory for obtaining sufficiently pure and undistorted PL spectra of the irradiated RPV steels.

An elegant solution to this problem has recently been suggested and examined in Ref. [3]. Its principle employs the fact that three γ-rays – one with energy of 1274 keV and two with 511 keV – are attributes of each event of positron annihilation, while only two γ-rays acompany every act of ^{60}Co decay. Precise enough selection of positron annihilation events out of all events observed is achieved by installing three γ-ray detectors and imposing a condition of triple coincidences. However, compared to conventional two-detector systems, the requirement of triple coincidences reduces drastically the rate of accumulation of PL spectra. It is thus evident that efficient enough γ-ray detectors have to be employed to make a three-detector setup viable. In addition, spectrometers with timing resolution power as good as 200 ps are needed to provide meaningful data on lifetimes of positrons in RPV steels, like in case of majority of metallic systems. These requirements are best satisfied by the BaF_2 scintilator detectors. Above all, these detectors display an advantageous property of excellent energy resolution power.

It is first necessary to determine the critical content of ^{60}Co prompt peak in PL spectrum at which the standard unfolding procedures fail to produce correct data on positron lifetimes and intensities. For this purpose we simulated a number of PL spectra of RPV steel and well-annealed α-Fe contaminated with different contributions of ^{60}Co. Analyses of these spectra in terms of lifetime components and corresponding intensities were performed with the aid of the unfolding procedure [4]. No measures for compensation of the ^{60}Co prompt peak were applied and at the same time this peak was fully neglected while analyzing the simulated spectra. The results obtained are given in details in the appendix.

It turns out that if the integrated contribution of prompt peak from ^{60}Co to the measured PL spectrum represents more than 1% of the total area of this spectrum the systematic uncertainty in determination of the α-Fe bulk lifetime will become comparable with a typical statistical uncertainty of this quantity. This critical contribution has been found under a realistic condition that the overall number of the accumulated events is 6.5×10^6. The other conditions imposed are specified in the appendix. Virtually the same quantitative conclusion regarding the ^{60}Co contamination has been obtained for simulated spectra of RPV steels.

Assume now a ^{22}Na positron source with a typical activity of 4 MBq and a two-detector system equipped with a pair of medium-sized BaF_2 crystals, as specified in the appendix. If such a system works in the fast–fast mode of operation, the found critical relative contribution of 1% will be reached with an α-Fe sample contaminated with ^{60}Co activity of ~ 0.1 MBq. In other words, if the ^{60}Co activity is higher than this value the role of the prompt peak in PL spectra cannot be neglected. On the other hand, compared to the simple case of α-Fe, the PL spectra obtained from a typical RPV steel sample display several PL components. Of them, the component belonging to the delocalized positrons is to be relatively weak and its lifetime should fall well below 100 ps. As a result, the critical ^{60}Co activity of RPV steel samples may be even lower than 0.1 MBq.

If the PL spectra yielded by two-detector system are not additionally corrected for the parasite ^{60}Co prompt peak, these spectra will not be acceptable for getting unbiased information on lifetimes of RPV steels with induced activity of ~ 0.1 MBq or higher. It is to be noted that this criterion rules out even the samples irradiated with unusually low neutron fluences. In view of the above-outlined difficulties with 'computational' elimination of the prompt peak the need for its instrumental suppression seems evident.

Within the present state-of-the-art of PL spectroscopy the way of suppressing the ^{60}Co prompt peak from PL spectra with the aid of a constraint of triple coincidences, as proposed in Ref. [3], is the best solution available so far. Unfortunately, to our knowledge the information from the literature about a practical use of this approach in the case of neutron irradiated materials is still missing.

The present paper describes a part of methodological results obtained within a broader project, devoted to investigation of RPV steels. A modification of the three-detector PL spectrometer of the type, proposed in Ref. [3], is given. The configuration of the modified spectrometer differs in some features from its original scheme. In particular, introduction of a more stringent energy condition for the second annihilation γ-ray, to the detriment of the time resolution for this γ-ray, is used for accumulating PL spectra free from parasite contribution of the ^{60}Co decay. Thanks to this the performance of the reported PL spectrometer makes it possible to extract unbiased information on positron lifetimes even from samples with unprecedent ^{60}Co activity of 4 MBq. As demonstrated in Sections 3 and 4, at this activity no noticeable traces of the ^{60}Co prompt peak in PL spectra have been observed, nor the influence of this possible peak on deduced lifetimes and intensities of the individual positron groups.

2. Three-detector spectrometer setup

In designing and building up the present three-detector spectrometer, we were guided by the experience we reached during completion and operating our two-detector BaF_2 systems [5–7]. Principal scheme of the present spectrometer is shown in Fig. 1. The two detectors referred below as the start and stop detector provide for timing information. Precise timing is in principle unnecessary for the second γ-ray. Thus, contrary to Ref. [3], the time resolution for the second annihilation γ-ray is reduced but fulfilling a more stringent condition on the energy, deposited by this γ-ray in the third detector, is required. Specifically, each triple coincidence in our system is embodied by the occurrence of a delayed coincidence of fast signals from the start and stop detectors and the simultaneous occurrence of a logic signal indicating detection of the second annihilation γ-ray with the required deposited energy in the vicinity of 511 keV photopeak. Hereafter, for the sake of brevity, the third detector is refered to as the energy detector.

BaF_2 scintillator crystals (S), purchased from the Karl Korth Kristalle, GmbH, Kiel, Germany,

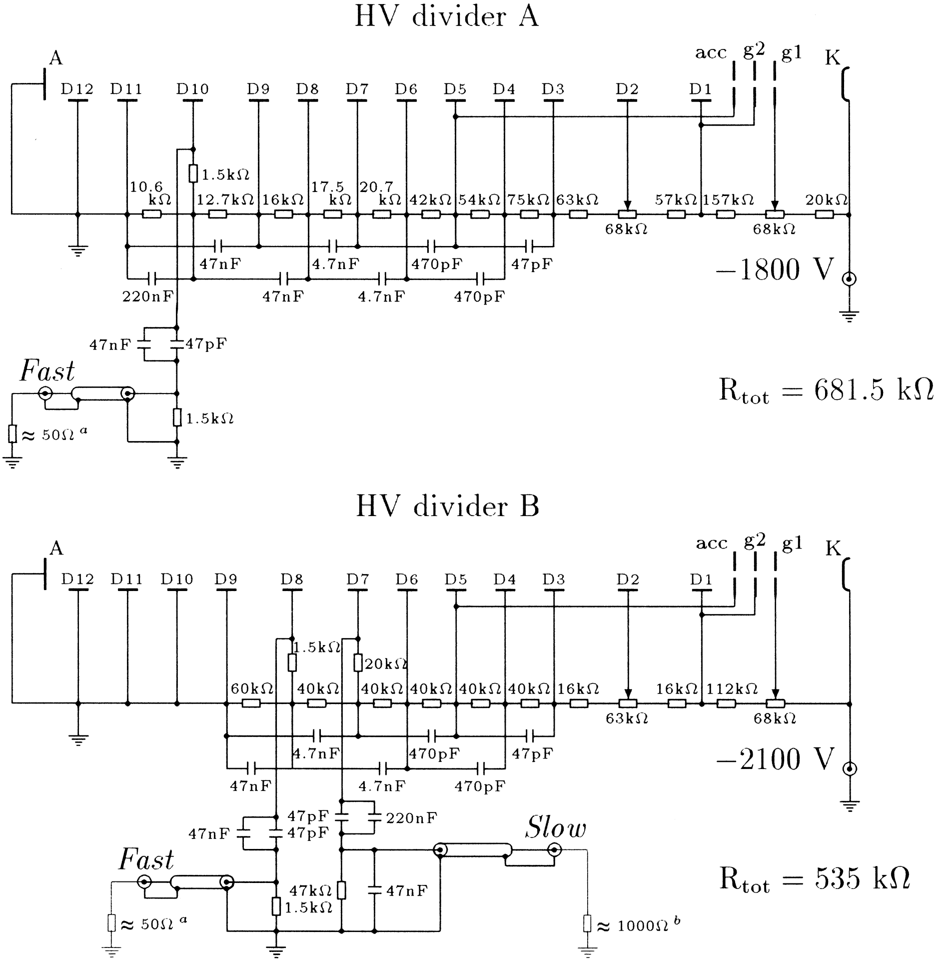

Fig. 1. A principal scheme of the HV dividers A and B. In case of divider B only the *Fast* output is used for the stop detector, while only the *Slow* output is used for the energy detector. PMT electrodes are denoted following to catalogue. R_{tot} stands for the total resistivity of the divider. Values labeled by *a* and *b* represent input impedances of a Constant-Fraction Differential Discriminator and a Spectroscopy Amplifier, respectively.

are used for γ-ray detection. Each crystal is optically coupled to a Philips XP2020/Q photomultiplier tube (PMT). The scintillator and the PMT of each detector are kept in a common housing, as described in Refs. [5,7]. Cylindrical scintillators with diameter of 25 mm and thickness of 12 mm are used in the start and energy detectors. Their axes intersect each other at angle of 90°. The stop detector is of a truncated conical shape with diameters of 25 and 40 mm and thickness of 25 mm. The stop and energy detectors are positioned face-to-face on a common axis of symmetry.

A ^{22}Na positron source of strength of ~ 4 MBq prepared on mylar foil following to the procedure [7] is utilized. The source–specimen sandwich is placed at the intersection of the axes of start and stop detectors. Distances of the detector faces from the sandwich position amount 2, 1.5 and 1.5 cm for the start, stop and energy detectors, respectively. A properly shaped cup made of Pb is put on the scintillator of the start detector (see Fig. 2) to prevent from false triple-coincidence events due to scattered γ-rays from the start detector to the energy or the stop detector, as well as from the energy

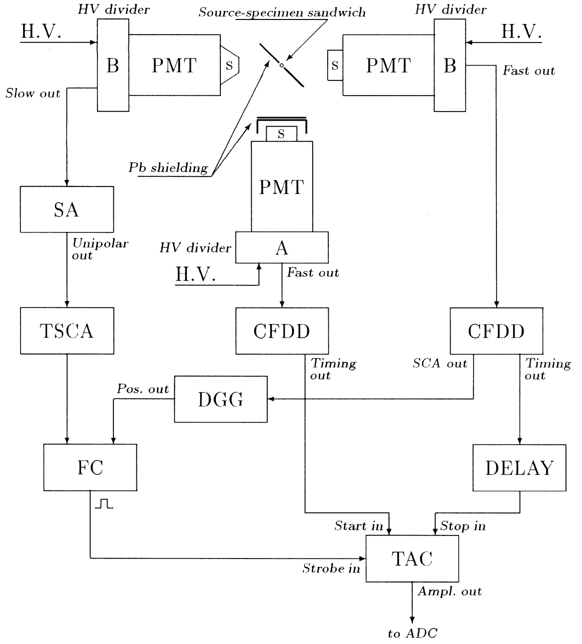

Fig. 2. A principal scheme of the three-detector positron-lifetime spectrometer. Abbreviations shown in the figure are explained in Section 2.

or the stop detector to the start detector. The thickness of the wall of the cup is 4 mm. The backscattering of γ-rays from the stop detector to the energy detector and vice versa is prevented by a 2 mm thick sheet of Pb positioned at the holder of the source-specimen sandwich. At the same time a circular hole made, 2 mm in diameter, at position of center of the source–specimen sandwich allows the γ-rays coming from the sample to reach the stop and energy detectors. Importance of this shielding have been proved by separate testing measurements with well-annealed α-Fe sample. Removing of the shielding in front of the start detector lead to shortening of the measured α-Fe bulk lifetime by about 2 ps, while removing of the shielding between the stop and the energy detectors caused increase of this lifetime by ~ 4 ps.

Following the another series of our testing measurements it became evident that a simultaneous use of two different types of HV dividers for the detector system was necessary to ensure the needed characteristics of the spectrometer. The schemes of these dividers, refered to as A and B, are shown in Fig. 1.

The start detector is equipped with the divider A. This divider is a slight modification of the HV divider IV, described in Ref. [7]. According to a serial number of 15553 the XP2020/Q PMT used in the start detector belongs to the same series of production of those PMTs for which the divider IV in Ref. [7] has originally been developed. However, unlike the PMTs reported in Ref. [7], the PMT of the start detector has been in use for a very limited period which implies that it displays a very high gain, typical for pristine PMTs. In these conditions, to prevent from saturation of the fast signal, the inter-dynode voltages provided by the divider A at the end of the dynode chain are lowered compared to the divider IV described in Ref. [7].

The remaining stop and energy detectors are equipped with PMTs of a newer series of production (their serial Nos. are 40403 and 41284, respectively) with a much higher gain than that of the PMT used in the start detector. Following to our testing measurements the divider IV, reported in Ref. [7], as well as the divider A turned out not to be optimum choices for these newer PMTs as with the use of both dividers we encountered problems with saturations and a non-linear response of the output signals. While solving similar problems authors in Ref. [8] found that shortening the dynode chain should reduce the effect of space charge as a primary cause of saturation and non-linearity. Guided by this conclusion and also by own experience with the spectrometer described in Ref. [7] we developed the tailored divider B.

With the divider B the distribution of the HV along the dynode chain is provided in the following manner: (i) an increased voltage is applied between the photocathode and the first dynode to ensure a high enough efficiency in collection of photoelectrons and to reduce their transit time spread; (ii) to minimize further the transit time spread the increased voltage is applied also between the successive two pairs of dynodes D1–D2 and D2–D3, as recommended for the sake of fast timing in Ref [8]; (iii) a minimum common interdynode voltage is applied between five successive pairs of dynodes within the segment of the chain D3–D8; (iv) a slightly increased voltage is applied between the pair of dynodes D8–D9 to reduce accumulation of the space charge in the vicinity of the dynode D8 from which the fast output signal is being taken.

The positive fast signal has to be inverted to provide the needed negative polarity at the input of a constant-fraction differential discriminator (CFDD). It is natural that with a shorter dynode chain the PMT gain becomes reduced. The amplitude of the fast output signal from the stop detector was still sufficient to excite the CFDD. In order to increase the signal-to-noise ratio at the input of the CFDD and invert this signal, we use a Hewlett-Packard MMIC high-frequency inverting preamplifier, Model MSA-0404 with a gain of 7.5 dB and an upper frequency limit of 2.7 GHz.

The slow signal is taken from the dynode D7. As can be seen from Fig. 1, this signal is streched using a passive RC circuit with $\tau = 50$ μs to meet the demands on the signal shape at the input of the spectroscopy amplifier (SA).

The fast output signals from the start and stop detectors are led to the input of a CFDD, ORTEC Model 583, see Fig. 2. The external clipping of the CFDDs was chosen as short as possible [7]. The timing output pulses from the CFDDs are led to the start and stop inputs of a time-to-amplitude converter (TAC), ORTEC Model 567. The TAC is strobed by the output from a fast coincidence unit (FC), ORTEC Model 414A, that is fed by the signals derived from the slow output from the energy detector and the fast output from the stop detector, see Fig. 2.

The slow output signal from the energy detector is amplified by a spectroscopy amplifier (SA), CANBERRA Model 2020 to feed a timing single channel analyser (TSCA), ORTEC Model 551. The TSCA is carefuly adjusted to select the 511 keV photopeak region. The TSCA positive output pulses are passed to the FC in which coincidence of these pulses with the positive pulses from the stop CFDD is checked. The latter pulses are delayed by means of a delay and gate generator (DGG), TENNELEC Model TC410A before arriving at the FC. The adjustment of the DGG for getting an optimum delay can be done using an auxiliary TAC that is started by the pulses from the DGG and stopped by the pulses from the TSCA. Adjustable resolving time of FC is selected to 100 ns. In case of higher ^{60}Co activities the resolving time may be easily decreased. As already mentioned, the output signal from the FC is used to strobe the TAC. In this way, the condition on triple coincidence between the start, stop and energy detector events is satisfied. Clearly, triple-coincidence mode may be easily changed to the 'normal' double coincidence mode by switching the TAC from external to internal strobing.

The amplitude output pulses from the TAC are transferred to a fast analog-to-digital converter (ADC), CANBERRA Model 8077. Data from the ADC are then stored in a memory of a PC which controls the data acquisition process in the way as described in Ref. [7].

3. Test measurements and results

The aim of test measurements performed with the present PL spectrometer was (i) to check that the PL spectrum of a well-known material is reproduced satisfactorily, independently of whether or not the sample contained ^{60}Co, (ii) to verify that the measured PL spectrum is free of shape distortions, and (iii) to determine the performance of the spectrometer, viz. the timing resolution power, the triple-coincidence count rate and degree of suppression of a ^{60}Co contribution. A well-recrystallized high-purity α-Fe was chosen as a reference material. The ^{22}Na positron source with activity of 4 MBq was tightly sandwiched between α-Fe discs with size of $10 \times 10 \times 0.3$ mm^3. Presence of the ^{60}Co in the specimens was mimicked by putting a ^{60}Co source at the positron source–specimen sandwich. Testing measurements were carried out at six different runs, denoted hereafter as A thru F, with a purpose to test the spectrometer under changing conditions and different modes of operation:

- the two-detector mode using pure α-Fe (run A),
- the three-detector mode, again with pure α-Fe (run B),
- the three-detector mode using pure α-Fe in combination with various ^{60}Co sources with activities of 0.7, 1.7 and 4 MBq (runs C, D and E, respectively), and

- the two-detector mode for the case of α-Fe combined with a ^{60}Co source with activity of 1.7 MBq (run F).

The PL spectra accumulated in these runs were decomposed using the maximum-likelihood procedure described in Ref. [4]. The results obtained are summarized in Table 1. The following quantities are included here: lifetime τ_1 of the first spectral component which corresponds to the α-Fe bulk positron lifetime in the case of no ^{60}Co influence, lifetimes τ_i and intensities I_i ($i = 2,3$) arise from annihilation of positrons in the source and covering foils, the total number of counts N_{tot} collected in the measured spectrum, the activity $A_{^{60}\mathrm{Co}}$ of ^{60}Co source added and, finally, the full-width at half-maximum (FWHM) of the timing-resolution function obtained from a fit. In the Table 1, quality of fits is characterized through the weighted sum of residuals χ^2, reduced to the number of degrees of freedom ν. In each run A–F, the three-component model with all the parameters left free provided good fits to the data. This is illustrated in Fig. 3 where PL spectrum measured in the run E is shown.

It follows from the Table 1 that in the two-detector (2D) mode the value of lifetime τ_1 reproduces

Table 1

Results of tests of the three-detector PL spectrometer. Meaning of the tabulated quantities is explained in the text. Experimental errors are given in parentheses in units of the last significant digit

Run	Mode	$A_{^{60}\mathrm{Co}}$ (MBq)	N_{tot} 10^6	χ^2/ν	τ_1 (ps)	τ_2 (ps)	I_2 (%)	τ_3 (ns)	I_3 (%)	FWHM (ps)
A	2D		3.0	1.01	107.6 (8)	380 (10)	7.5 (3)	1.4 (1)	1.0 (1)	208
B	3D		2.4	0.98	108.6 (8)	390 (10)	7.7 (3)	1.8 (2)	0.73 (7)	217
C	3D	0.7	1.0	0.97	108 (2)	400 (20)	7.7 (5)	2.1 (2)	1.3 (1)	222
D	3D	1.7	1.0	1.00	108 (1)	400 (30)	6.9 (4)	1.8 (4)	0.7 (2)	224
E	3D	4.0	2.5	0.99	109 (1)	370 (20)	8.4 (4)	2.2 (3)	0.92 (8)	224
F	2D	1.7	1.7	1.05	104 (1)	350 (30)	7.4 (6)	1.3 (2)	0.9 (2)	227

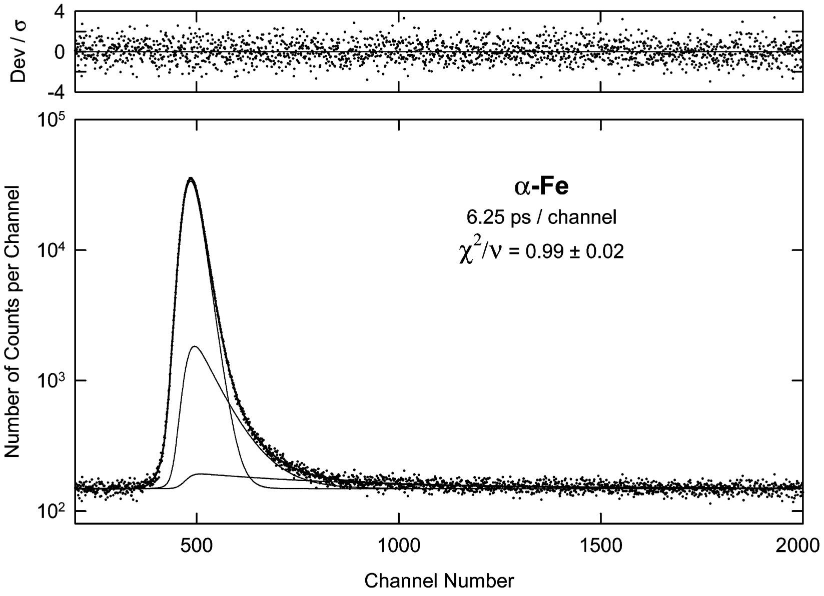

Fig. 3. Positron-lifetime spectrum of α-Fe with ^{60}Co source of activity 4 MBq added (lower panel). The spectrum was measured in the 3D mode (run E in Table 1). The weighted residuals (upper panel) indicate the quality of the fit.

well our value 108.1 ± 0.1 ps, determined previously using the conventional fast–slow setup [7], as well as the value 107.9 ± 0.2 ps that was obtained from measurements with the fast–fast system based on the use of the energy summing technique for energy selection of coincidence events [6]. The 2D measurement clearly demonstrates the effect of the ^{60}Co prompt peak which is expressed by apparent shortening of τ_1, see results for run F in Table 1. Knowing activities of ^{60}Co and ^{22}Na, as well as peak-to-Compton ratios we have estimated the fraction x of ^{60}Co contribution in the measured spectrum to be 20% in run F. Simulations performed in the appendix revealed that shortening of τ_1 to 104 ps corresponds to $x = 19\%$, which is in a good agreement with our estimate. The presence of ^{60}Co promt-peak contribution in the spectrum in run F is reflected also by a worsened value of χ^2/ν. On the other hand, three-detector (3D) measurements with different contents of ^{60}Co activity added (runs B–E) exhibit no effect of the ^{60}Co prompt peak. All the measured values of τ_1 agree within the quoted experimental errors with the above-mentioned value of τ_{bulk}. A typical coincidence count rate in the 3D mode was around 15 s^{-1}. Timing resolution found, ~ 220 ps (FWHM), is considerably better than that reported for the three-detector spectrometer in Ref. [3]. A slightly better timing resolution in run A is a consequence of narrower energy windows of CFDDs in this run compared to all the other ones. Gradual worsening of timing resolution of the spectrometer with increasing ^{60}Co activity may be seen in Table 1. It is a consequence of the pile-up effects due to the increasing total load of the electronics system. The similar effect was also reported in Ref. [3].

On the basis of simulations performed in the appendix, it can be concluded from the results of test runs C–E that the integral contribution of the ^{60}Co prompt peak to the measured PL spectra is supressed fairly below 1%. The relevant characteristics of the present spectrometer is represented by the values of factor $Q = c(\text{3D})/c(\text{2D})$, characterizing the relative suppresion of the coincidence count rate c when the spectrometer is switched from 2D to 3D mode of operation. For the case when only the ^{22}Na positron source with activity of 4 MBq was located at measuring position we found $Q(^{22}\text{Na}) = 0.33$. When this source was replaced by the ^{60}Co source with activity of 1.7 MBq we observed a more pronounced suppresion, characterized by $Q(^{60}\text{Co}) = 0.0017$. It is thus expected that in real conditions, when specimens studied contain a given ^{60}Co activity, the onset of the 3D mode operation suppresses the coincidence rate of the parasite prompt peak 190-times stronger than the overall effect due to positron annihilation. It is to be noted that the number of coincidences originating from a ^{22}Na source is proportional to the source activity both in 2D and 3D mode. On the other hand, the coincidence count rate for ^{60}Co source is proportional to the source activity in 2D mode only. In the case of 3D mode the coincidences originating from ^{60}Co source represent mainly such events when the two time-correlated γ-rays, emitted by ^{60}Co are detected by the start and the stop detectors, while another γ-ray, which is not correlated with the previous two is intercepted by the energy detector. This is, indeed, possible due to the Compton scattering that occurs in the stop and the energy detectors, as this scattering may leave in these detectors energies falling within the adjusted energy windows. With this simplified picture the coincidence count rate, belonging to the ^{60}Co prompt peak in the 3D mode of operation, is expected to be proportional to the square of the ^{60}Co activity. Consequently, the ratio $Q(^{22}\text{Na})/Q(^{60}\text{Co})$ is to be inversely proportional to this activity.

For purpose of comparison with Ref. [3] we note that in the case of a source with ^{60}Co activity of 1.85 MBq the value of this ratio turned out to be $Q(^{22}\text{Na})/Q(^{60}\text{Co}) = 180$. This value is to be compared with $Q(^{22}\text{Na})/Q(^{60}\text{Co}) = 100$ that was achieved with the three-detector PL spectrometer, reported in Ref. [3]. The present spectrometer thus provides ~ 1.8 times better suppresion of ^{60}Co prompt peak compared to that described in Ref. [3]. This increase of ^{60}Co prompt peak suppression is likely caused by the following factors: (i) the use of the precise energy selection of one of annihilation γ-rays in the energy detector, (ii) the use of the lead shielding which reduces number of false triple-coincidence events connected with γ-rays scattered in one of the detectors (see Section 2). In addition, the ratio $Q(^{22}\text{Na})/Q(^{60}\text{Co})$ may be slightly influenced by the resolving time of FC (see

Section 2). Decreasing of the width of time window of FC reduces the value $Q(^{60}\text{Co})$ as it suppressed the number of false triple-coincidences when the two time correlated γ-rays from ^{60}Co source are detected by the start and stop detectors and another γ-ray which is not time correlated with the previous ones is detected in the energy detector. This effect is, however, more important in the case of real measurement when ^{60}Co and ^{22}Na sources are placed simultaneously in the source-sample sandwich, as it will be discussed below. However, following our testing measurements with a provisional version of the reported PL spectrometer, the main positive impact of the introduced energy selection is virtually full absence of parasite structures in measured PL spectra, even in conditions of high activities of ^{60}Co.

It should be pointed out that under the condition of real measurement, when ^{22}Na source is sealed between a pair of samples containing the ^{60}Co activity, the suppression of the ^{60}Co prompt peak will be smaller then that indicated by value of $Q(^{60}\text{Co})$. This reflects the fact that when the two time-correlated γ-rays emited by ^{60}Co source are detected by the start and the stop detector, another γ-ray originating from ^{22}Na source may be detected by the energy detector during the time interval required by FC for a coincidence. Nevertheless the ratio $Q(^{22}\text{Na})/Q(^{60}\text{Co})$ represents well-defined quantity which may be used as a benchmark for comparison of efficiency of various spectrometers in instrumental suppression of the ^{60}Co prompt peak contribution.

4. The use of the spectrometer for studying RPV steels

In order to demonstrate practical applicability of the reported three-detector spectrometer in investigations of neutron-irradiated steels, we undertook measurements on samples of VVER-440 type RPV steel 15Kh2MFA. The specimens were irradiated to various fluences Φ in VVER-440/213C light water reactor. Temperature of irradiation was $\approx 270°\text{C}$ and the fast neutron flux was $\approx 4 \times 10^{16}\ \text{m}^{-2}\ \text{s}^{-1}$. The specimens irradiated to an intermediate fluence of $3 \times 10^{24}\ \text{m}^{-2}$ (sample B, 3 years of irradiation) and the other one irradiated to maximum fluence of $10^{25}\ \text{m}^{-2}$ (sample A, 10 years of irradiation) were selected from the series of specimens irradiated to various fluences to demonstrate the performance of the spectrometer. Detailed description of this investigation and obtained results will be presented in Ref. [9]. The round-shape specimens with diameter of 8 mm and thickness of 0.25 mm were prepared from fractured Charpy-V bodies. Surfaces of all the specimens were carefully mechanically ground and polished and chemically mechanically polished in the final step to minimize the preparation-induced stresses. It was shown [10] that defects which may be induced into the specimens by their cutting are completely removed by this procedure.

We have found that PL spectrum of the sample A is well fitted by two exponential components, except for two components belonging to a source contribution. The PL spectrum for this sample and the fitted model function is shown in Fig. 4 Weighted residuals shown on upper panel of the Fig. 4 indicate good quality of the fit. On the other hand, three components are needed for achieving a good-quality fit in the case of sample B. The lifetimes and relative intensities for samples A and B are shown in Table 2. The result of two-component fit for the non-irradiated sample, denoted as C, of the same type of RPV steel performed in Ref. [10] is shown in the last row of Table 2 for comparison. The two-component source contribution, which was the same for all the samples, is not included in the table.

The value of χ^2 per degree of freedom, the number of counts in the spectrum N_c and the ^{60}Co activity of the pair of samples are also listed in Table 2.

Detailed discussion of the results is out of scope of this paper and we therefore limit ourselves to a few remarks. For detailed discussion of the results see Ref. [9]. It is natural to assume that the shortest component τ_1 arises from annihilations of the delocalized positrons while the components τ_2 and τ_3 represent contribution of positrons trapped at defects.

Clearly, within the achieved precision the lifetime $\tau_2 \sim 150$ ps remains the same for all the samples. Analysis in Ref. [10] has revealed that this

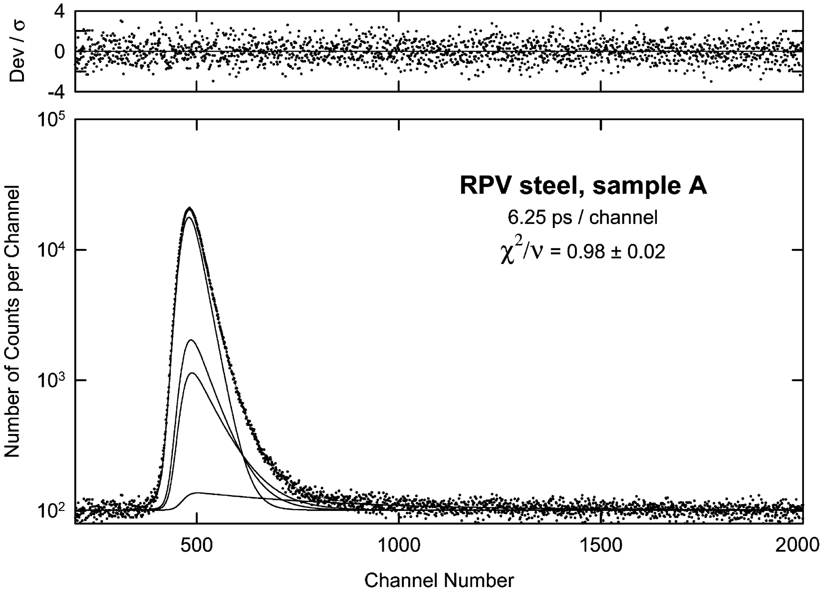

Fig. 4. Positron-lifetime spectrum of VVER-440 type RPV steel 15Kh2MFA irradiated to fluence $\Phi = 9.96\times10^{24}$ m^{-2} (sample A). The pair of samples contains 4 MBq of ^{60}Co activity. The spectrum was measured in the 3D mode.The weighted residuals (upper panel) indicate the quality of the fit.

Table 2
Results of PL study of VVER-440 type RPV steel 15Kh2MFA. Irradiated specimens (A, B) were measured using the reported three-detector spectrometer. The results for non-irradiated sample C was taken from Ref. [10]. Meaning of the tabulated quantities is explained in the text. Experimental errors are given in parentheses in units of the last significant digit

Sample	Φ (10^{24} m^{-2})	τ_1 (ps)	I_1 (%)	τ_2 (ps)	I_2 (%)	τ_3 (ps)	I_3 (%)	χ^2/ν	N_c (10^6)	$A_{^{60}Co}$ (MBq)
A	9.96	—	—	149.3 (7)	87 (4)	260 (30)	13 (4)	0.977	1.7	4
B	3.32	50 (10)	9 (3)	148 (9)	81 (7)	250 (30)	10 (5)	1.010	6.2	1
C	0	64 (5)	14.1 (7)	151.6 (8)	85.9 (6)	–	–	1.012	18.5	0

component comes from positrons trapped at dislocations which are present in the material already prior to irradiation.

Irradiation of the samples leads to creation of new types of defects in the material. It is reflected by the occurrence of component τ_3 which is not present in the non-irradiated sample. Lifetime of this component indicates that these defects may be attributed to small vacancy clusters containing 5–6 vacancies [11]. In the case of sample A no component belonging to delocalized positrons has been found in the PL spectrum. Virtually all positrons thus annihilate as trapped at dislocations or irradiation-induced clusters in this sample. It corresponds with expected increasing number of irradiation-induced defects with increasing fluence.

It has to be emphasized that no detectable distortions were found in all measured spectra. In addition, very good agreement of the lifetime τ_2 was obtained from irradiated samples using the three-detector spectrometer with that of non-irradiated sample measured by conventional two-detector device in Ref. [10]. Both these findings represent undirect but strong evidence for reliability of the spectrometer to suppress efficiently the ^{60}Co parasite prompt peak contribution.

5. Conclusions

The three-detector PL spectrometer equipped with the BaF_2 scintillators has been built up for the needs of studying defects in neutron-irradiated RPV steels. Precise energy information about one of the annihilaton γ-rays obtained from the slow PMT signal is used to derive the triple coincidence condition. Three important characteristics were achieved:

- the timing resolution of 220 ps,
- the coincidence count rate of 15 s^{-1} for a 4 MBq ^{22}Na source, and
- the suppression ratio $Q(^{22}\mathrm{Na})/Q(^{60}\mathrm{Co}) = 190$ for activity of ^{60}Co of 1.7 MBq.

As an example of practical use of the spectrometer, results obtained from measurements with irradiated VVER-440-type RPV steel samples were presented. These results, as well as those from auxiliary measurements with composite samples of α-Fe and ^{60}Co clearly demonstrated that the PL spectra produced by the spectrometer are free from any detectable distortions, even at ^{60}Co activities of 4 MBq, which is considered to be the most valuable characteristic in the design of the reported spectrometer.

Owing to all these achieved characteristics we could use the reported three-detector spectrometer for the study of defects in RPV samples, exposed to neutron fluences ranging up to 10^{25} m^{-2} [9]. This quoted study represents probably the first case of application of a three-detector PL spectrometer to the task for which it had been originally devised. To give a credit to the authors in Ref. [3], it is to be stressed that the idea of imposing a triple-coincidence condition in PL measurements in samples contamined by ^{60}Co has turned out to be very successful.

Acknowledgements

Authors are indebted to Dr. Jan Kočík and Dr. Eliška Keilová from NRI Řež plc for preparation of irradiated RPV specimens. This work was financially supported by the Grant Agency of the Czech Republic under contract No. 106/96/1319.

Appendix

Series of computer-simulated PL spectra were carried out to investigate quantitatively the conditions under which the role of the ^{60}Co prompt peak in PL spectra can be neglected. The simulated spectra were assumed to contain N exponential components and a ^{60}Co prompt-peak contribution. The prompt-peak was considered to be of the same shape as the time-resolution function. All the simulated spectra contained 6.5×10^6 counts and they were analyzed in the same manner as real experimental spectra. The timing resolution function was kept fixed in all the fits.

As a first step, three-component model spectra ($N = 3$) formed by components with lifetimes 108, 368 and 1500 ps and relative intensities 92%, 7% and 1%, respectively, were simulated. Such spectra resemble those for a recrystallized α-Fe sample in testing measurements, see Section 3. The resolution function with FWHM of 220 ps was assumed, which corresponds to conditions in real measurements as described in Sections 3 and 4. Five independent spectra were simulated using identical input parameters which made it possible to obtain the errors both from the fit and from the spread of values of the fitted parameters. The lifetime τ_1 deduced from the decomposition of the simulated spectra as a function of the relative size of the ^{60}Co contribution to the spectrum is plotted in Fig. 5. Clearly, decrease of τ_1 by one standard deviation occurs for a 1% ^{60}Co fraction in the spectrum. Difference $\tau_{av}(0) - \tau_{av}(x)$ of average lifetimes of a simulated α-Fe spectrum with no ^{60}Co contribution and that with x% of ^{60}Co contribution is also plotted in Fig. 5. This parameter is less sensitive to x then τ_1 as the increase by one standard deviation occurs at $x \approx 3\%$. We thus conclude that any contribution of the ^{60}Co prompt peak to the PL spectrum that exceeds 1% appears to have statistically meanigful influence on parameters obtained from the standard decomposition of PL spectrum for the α-Fe samples.

As a next step, simulations of PL spectra of irradiated RPV steel were performed. Three-component model spectra with lifetimes of 30, 150 and 260 ps and relative intensities of 11%, 78% and 11%, respectively, were simulated. The same resolution function as in the previous case was used. A similar kind of spectrum is expected for irradiated RPV steels, as indicated by observations in Ref. [12]. The first component ($\tau_1 = 30$ ps) represents a contribution of delocalized positrons, the second one ($\tau_2 = 150$ ps) comes from positrons trapped at dislocations [10] and the last one ($\tau_3 = 260$ ps) belongs to a contribution of positrons trapped in irradiation-induced vacancy clusters. Long-lived components arising from annihilations in the source and its covering foils were not included in the simulated spectra as they are expected to be less influenced by ^{60}Co prompt-peak. The errors of fitted parameters were obtained in the same way as in the previous case of α-Fe spectra. The lifetimes τ_2 and τ_3 were fixed in order to suppress uncertainties of the remaining fitted parameters. The difference $\tau_{av}(0) - \tau_{av}(x)$ of average lifetimes of the simulated spectrum for RPV steel with no ^{60}Co contribution and that with x% of ^{60}Co is shown in Fig. 6. The lifetime τ_1 and the relative intensities I_1 and I_2 of the corresponding components of simulated spectra for RPV steel are shown in Fig. 6 as a functions of x. It is clear from the Fig. 6 that the ^{60}Co prompt peak contribution in the spectrum exceeding 1% leads to statistically meaningful changes in the lifetime τ_1 and relative intensities. Similar behavior is exhibited also by the difference of the average lifetimes in Fig. 6.

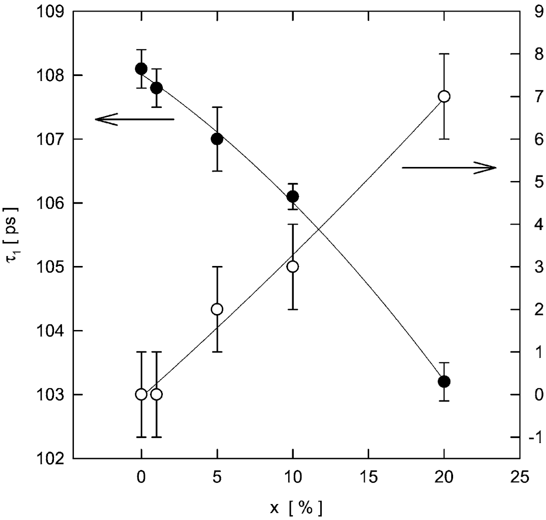

Fig. 5. Dependence of positron lifetime τ_1 obtained from fit of simulated spectra of α-Fe on fraction x of ^{60}Co in the spectrum. Moreover difference $\tau_{av}(0) - \tau_{av}(x)$ of average lifetimes of the spectrum with no ^{60}Co contribution and those with x% of ^{60}Co contribution is plotted.

We conclude that ^{60}Co fractions in spectra below 1% are required in order to ensure unbiased

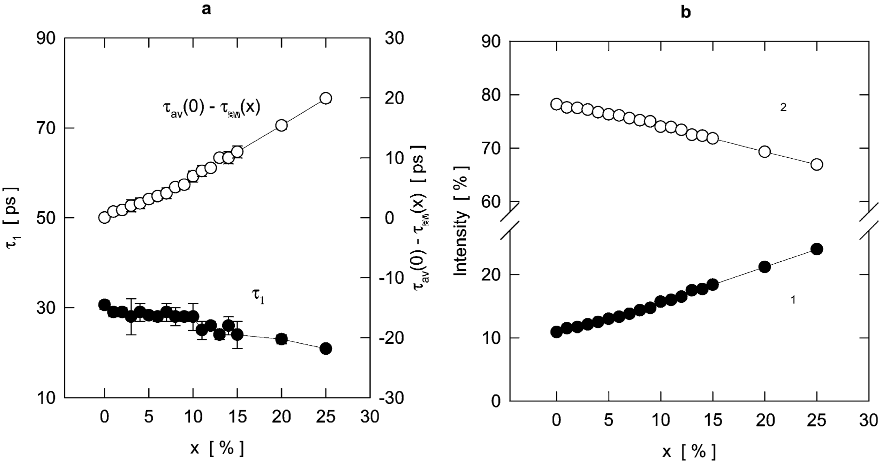

Fig. 6. (a) Dependence of positron lifetime τ_1 obtained from fits of simulated spectra for RPV steel on a fraction x of ^{60}Co prompt peak contribution to the spectra. Also the difference $\tau_{av}(0) - \tau_{av}(x)$ of the average lifetimes of the spectrum with no ^{60}Co contribution and that with x% of ^{60}Co contribution is plotted. (b) Relative intensities I_1 and I_2 obtained from fits of simulated spectra as a function of x.

lifetimes and relative intensities for spectral components both in the case of defect-free α-Fe and the irradiated RPV steel samples.

References

[1] M. Valo, R. Krause, K. Saarinen, P. Hautojärvi, J. Russel Hawtorne, in: R.E. Stoller, A.S. Kumar, D.S. Gelles (Eds.), Effects of Radiation Materials: 15th Int. Symp., ASTM STP 1125, American Society for Testing and Materials, Philadelphia, 1992, p. 172.

[2] G.H. Dai, P. Moser, J.C. Van Duysen, Mater. Sci. Forum 105–110 (1992) 941.

[3] L. Van Hoorebeke, A. Fabry, E. van Walle, J. Van de Velde, D. Segers, L. Dorikens Vanpraet, Nucl. Instr. and Meth. A 371 (1996) 566.

[4] I. Procházka, I. Novotný, F. Bečvář, Mater. Sci. Forum 255–257 (1997) 772.

[5] F. Bečvář, L. Lešták, I. Novotný, I. Procházka, J. Vrzal, F. Šebesta, Mater. Sci. Forum 175–178 (1995) 947.

[6] F. Bečvář, J. Čížek, I. Procházka, Acta Phys. Polonica A 95 (1999) 448.

[7] F. Bečvář, J. Čížek, L. Lešták, I. Novotný, I. Procházka, F. Šebesta, Nucl. Instr. and Meth. A 443 (2000) 557.

[8] M. Moszyński, Nucl. Instr. and Meth. A 337 (1993) 154.

[9] J. Kočík, E. Keilová, J. Čížek, I. Procházka, J. Nucl. Mater., submitted for publication.

[10] J. Čížek, I. Procházka, J. Kočík, E. Keilová, Phys. Stat. Sol. A, accepted for publication.

[11] A. Hempel, M. Saneyasu, Z. Tang, M. Hasegawa, G. Brauer, A. Plazaola, S. Yamaguchi, in: M.L. Hamilton, A.S. Kumar, S.T. Rosinski, M.L. Grossbeck (Eds.), Effects of Radiation on Materials: 19th International Symposium ASTM STP 1366, American Society for Testing and Materials, Philadelphia, 1999.

[12] C. Lopes Gil, A.P. De Lima, N. Ayres De Campos, J.V. Fernandes, G. Kögel, P. Sperr, W. Triftshäuser, D. Pachur, J. Nucl. Mater. 161 (1989) 1.